



THE UNIVERSITY *of* EDINBURGH

Edinburgh Research Explorer

Unified theory of global flow and squirt flow in cracked porous media

Citation for published version:

Jakobsen, M & Chapman, M 2009, 'Unified theory of global flow and squirt flow in cracked porous media', *Geophysics*, vol. 74, no. 2, pp. WA65-WA76. <https://doi.org/10.1190/1.3078404>

Digital Object Identifier (DOI):

[10.1190/1.3078404](https://doi.org/10.1190/1.3078404)

Link:

[Link to publication record in Edinburgh Research Explorer](#)

Document Version:

Publisher's PDF, also known as Version of record

Published In:

Geophysics

Publisher Rights Statement:

Published in *Geophysics* by the Society of Exploration Geophysicists (2009)

General rights

Copyright for the publications made accessible via the Edinburgh Research Explorer is retained by the author(s) and / or other copyright owners and it is a condition of accessing these publications that users recognise and abide by the legal requirements associated with these rights.

Take down policy

The University of Edinburgh has made every reasonable effort to ensure that Edinburgh Research Explorer content complies with UK legislation. If you believe that the public display of this file breaches copyright please contact openaccess@ed.ac.uk providing details, and we will remove access to the work immediately and investigate your claim.



Publisher PDF- Deposited in Edinburgh University Research Archive. Copyright (2009) Society of Exploration Geophysicists.

Cite As: Jakobsen, M & Chapman, M 2009, 'Unified theory of global flow and squirt flow in cracked porous media' *Geophysics*, vol 74, no. 2, pp. WA65-WA76. DOI: 10.1190/1.3078404

Unified theory of global flow and squirt flow in cracked porous media

Morten Jakobsen¹ and Mark Chapman²

ABSTRACT

Approximations for frequency-dependent and complex-valued effective stiffness tensors of cracked porous media (saturated with a single fluid) are developed on the basis of an inclusion-based model (the T-matrix approach to rock physics) and a unified treatment of the global-flow and squirt-flow mechanisms. Essentially, this study corrects an inconsistency or error related to fluid-mass conservation in an existing expression for the t-matrix (wave-induced deformation) of a communicating cavity, a cavity that is isolated with respect to stress propagation (through the solid matrix) but that can exchange fluid mass with other cavities because of global and/or local pressure gradients associated with passage of a long viscoelastic wave. An earlier demonstration of Gassmann consistency remains valid because the new theory of global flow and squirt flow (which also takes into account solid mechanical effects of stress interaction by us-

ing products of communicating t-matrices associated with two-point correlation functions of ellipsoidal symmetry) only differs from an earlier version by a correction term that goes to zero in the low-frequency limit. If the unified model is applied to the special case of a model involving a single set of spheroidal cavities (having the same aspect ratio and orientation), the results become identical with those obtained using a special theory of global flow that predicts that at zero frequency the cavities will behave as though they are isolated with respect to wave-induced fluid flow (in accordance with Gassmann's formulas) and that at high frequencies, they will behave as though they are dry. Our theory predicts that there will be a continuous transition from a global-flow-dominated system (characterized by a negative velocity dispersion) to a squirt-flow-dominated system (characterized by a positive velocity dispersion) if one begins with a single set of cavities and then introduces a distribution of shapes and/or orientations that gradually becomes wider (more realistic).

INTRODUCTION

Overall properties of cracked porous media

When an acoustic wave propagates in a cracked porous medium, the wavelength often is much larger than the microstructure's scale size, so that the wave can "see" only an averaged or homogenized structure and not the individual pores and cracks. Therefore, for acoustic or seismic modeling, the cracked porous medium can be replaced by a long-wavelength, equivalent homogeneous medium that can be both anisotropic and viscoelastic because of microstructural alignments and wave-induced fluid flow, respectively.

In models of real media that are both anisotropic and viscoelastic, the stress tensor is given by a convolution of the (time-dependent) effective stiffness tensor with the strain tensor (Carcione, 2007). Taking the Fourier transform of this convolution integral, we obtain the usual stress-strain relation (Hooke's law), but with a frequency-

dependent and complex-valued effective stiffness tensor (Carcione, 2007). In this paper, approximations for the frequency-dependent and complex-valued effective stiffness tensors of cracked porous media (that are completely saturated with a single fluid) are developed on the basis of an inclusion-based model (the T-matrix approach of Jakobsen et al. [2003a]) and a unified treatment of the global-flow and squirt-flow mechanisms that allows for microstructural alignments.

Essentially, our paper corrects an inconsistency or error (related to the coupling between the global- and squirt-flow processes because of fluid-mass conservation) in the inclusion-based model for wave-induced fluid flow developed by Jakobsen et al. (2003b). The existence of an error in the theory of Jakobsen et al. (2003b) is serious because the theory of Jakobsen et al. (2003b) contains the frequently cited theory of nonidentical communicating cracks (nonintersecting but interconnected through seismically transparent channels and

Manuscript received by the Editor 31 March 2008; revised manuscript received 1 October 2008; published online 11 March 2009.

¹University of Bergen, Department of Earth Science and Centre for Integrated Petroleum Research, Bergen, Norway. E-mail: morten.jakobsen@geo.uib.no.

²British Geological Survey, Edinburgh Anisotropy Project, Edinburgh, Scotland. E-mail: mhch@bgs.ac.uk.

© 2009 Society of Exploration Geophysicists. All rights reserved.

characterized by different orientations and/or shapes and aspect ratios) developed by Hudson et al. (1996), Pointer et al. (2000), and Tod (2001) as a special case. (See Jakobsen and Hudson [2003] for a generalization and comparison of the T-matrix approach of Jakobsen et al. [2003a] to Hudson's crack model.) Before we become more technical, we will first discuss the phenomenon of wave-induced fluid flow (at different scales) more generally.

Qualitative description of global flow and squirt flow

Global flow is caused by pressure gradients at the scale of the acoustic wavelength and in the direction of wave propagation, whereas squirt flow is caused by pressure gradients at the scale of the microstructure and in directions that potentially are different from that of wave propagation. As Figure 1 illustrates, squirt flow occurs within a representative volume element (RVE) that contains many pores and cracks, and the RVE appears as a point at the macroscale, in accordance with the continuum hypothesis. If the RVE contains a single set of cavities (characterized by the same shape and orientation), then all the different cavities will have the same wave-induced change in pore-fluid pressure, so that only global flow will occur. When the introduction of small perturbations in the microstructure generates local pressure gradients, squirt flow in the direction of the local pressure gradients (e.g., from cracks to pores and/or between cracks of different orientations) will occur within the RVE, in addition to the global flow in and out of the RVE and in the direction of wave propagation. Global- and squirt-flow processes are associated with different characteristic times but are coupled to each other through fluid-mass conservation, suggesting a need to correct for the effects of global flow in and out of the RVE before trying to model the change in fluid mass within a particular set of cavities (pores or cracks) inside the RVE.

Mathematical models of global flow and/or squirt flow

Historically, many have attempted to develop special theories of global flow (Biot, 1956, 1962; Hudson et al., 1996), special theories of squirt flow (Mavko and Nur, 1975; O'Connell and Budiansky, 1977; Mavko and Jizba, 1991; Mukerji and Mavko, 1994; Dvorkin

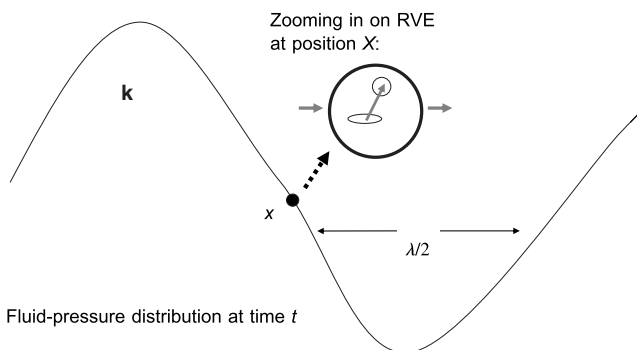


Figure 1. The phenomenon of wave-induced fluid flow illustrated for a time-harmonic plane wave propagating in a cracked porous medium. Arrows in the direction of wave propagation and in other directions denote global flow and squirt flow, respectively. The squirt flow will disappear if all cavities (pores and cracks within the RVE) are identical, i.e., have the same shape and orientation. Also, the pressure inside each cavity (within each set of cavities) must be equal to ensure statistical homogeneity needed for using effective-medium theory.

et al., 1995; Chapman, 2003), and unified theories of global flow and squirt flow (Dvorkin and Nur, 1993; Hudson et al., 1996; Chapman et al., 2002; Jakobsen et al., 2003b; Jakobsen and Hudson, 2003; Jakobsen, 2004). Existing theories of global and/or squirt flow can be divided into two categories. One category is phenomenological theories in which the model parameters are empirical and are not related directly to the details of the microstructure (Biot, 1956, 1962; Dvorkin and Nur, 1993; Mavko and Jizba, 1991; Mukerji and Mavko, 1994; Dvorkin et al., 1995). The second category is inclusion-based models that typically are based on the result of Eshelby (1957) or Mura (1982) for the response of a single ellipsoidal inclusion within an infinite, homogeneous matrix from a homogeneous applied stress at infinity (Mavko and Nur, 1975; O'Connell and Budiansky, 1977; Hudson et al., 1996; Jakobsen et al., 2003b; Jakobsen and Hudson, 2003; Jakobsen, 2004; Chapman et al., 2002; Chapman, 2003). The phenomenological approach that Biot (1956) pioneered might be attractive when dealing only with global flow, but when squirt flow is included (which represents an example of a coupled process sensitive to the details of the microstructure), the inclusion-based approach is more attractive.

All the theories listed above are based on certain simplifying assumptions that tend to restrict their range of validity, and some of them contain inconsistencies or errors. For example, the theories of Biot (1956), Mavko and Nur (1975), O'Connell and Budiansky (1977), Mavko and Jizba (1991), Dvorkin et al. (1995), Dvorkin and Nur (1993), and Chapman et al. (2002) are based on the assumption of (poro)elastic isotropy, whereas the theories of Biot (1962), Mukerji and Mavko (1994), Hudson et al. (1996), Chapman (2003), Jakobsen et al. (2003b), Jakobsen and Hudson (2003), and Jakobsen (2004) allow for anisotropy (microstructural alignments). The so-called BISQ (Biot + squirt) model of Dvorkin and Nur (1993) is inconsistent with the relations of Gassmann (1951) between the dry and undrained elastic moduli. Also, the squirt-flow models of Mavko and Jizba (1991) and Mukerji and Mavko (1994) focus only on the high-frequency limit. Among the inclusion-based models referred to above, the T-matrix approach of Jakobsen et al. (2003a, 2003b) (or of Jakobsen and Hudson [2003]) represents the most general model because it allows for nondilute (relatively large) concentrations of (nonintersecting) cavities (pores, cracks) that are characterized by many different shapes, orientations, and spatial distributions and that can communicate through the exchange of fluid mass in a network of seismically transparent channels (Hudson et al., 1996; Chapman, et al., 2002).

In other words, the T-matrix approach of Jakobsen et al. (2003a, 2003b) is a generalization of Hudson et al.'s (1996) model for communicating nonidentical cracks because the T-matrix approach (but not Hudson et al.'s crack model) allows for a finite storage porosity and nondilute (higher) crack densities. In addition, expansion of the T-matrix approach to first order in the inclusion concentrations gives the same result as Chapman's (2003) special theory of squirt flow in models for fractured reservoirs involving spherical pores, randomly oriented microcracks, and fully aligned mesocracks, if global-flow effects are ignored and characteristic times for squirt flow at different scales are modified as discussed by Agersborg et al. (2007). (Jakobsen and Hudson's (2003) 4D T-matrix approach is more general in principle than Jakobsen et al.'s (2003b) 3D T-matrix approach because it takes into account (inertial effects beyond the long-wavelength approximation) scattering attenuation as well as attenuation from wave-induced fluid flow. However, the more-dynamic theory

of [Jakobsen and Hudson \[2003\]](#) so far has been evaluated only in the long-wavelength limit, where it produces the same results as the theory of [Jakobsen et al. \[2003b\]](#).)

Inconsistent models of identical and nonidentical cavities

[Jakobsen et al. \(2003b\)](#) (and [Jakobsen and Hudson \[2003\]](#)) followed [Hudson et al. \(1996\)](#) in using an ansatz for the mass flow out of each cavity set, which originally was believed to be consistent with fluid-mass conservation. However, that [Hudson et al.'s \(1996\)](#) theories for a single set and multiple sets of (nonidentical) communicating cracks are not consistent with each other (as pointed out by [Tod \[2001\]](#) and [Chapman et al. \[2002\]](#)) suggests that the theories of [Hudson et al. \(1996\)](#) and [Jakobsen et al. \(2003b\)](#) are not consistent with the principle of fluid-mass conservation. Because the models of identical and nonidentical cracks developed by [Hudson et al. \(1996\)](#) are not consistent with each other, it is clear that at least one of these models must be wrong. For a single set of cracks, all cracks by definition will have the same shape and orientation, so that there cannot be squirt flow because of a lack of local pressure gradients. Nevertheless, the theory for multiple sets of cracks (but not the theory for a single set) predicts that the velocity dispersion depends on the characteristic time for squirt flow ([Tod, 2001](#), p. 253).

The single-set and multiple-set theories both predict that (in a model involving only a single set of fully aligned cracks), at very low frequencies the cracks will behave as though they are isolated with respect to wave-induced fluid flow. However the single-set theory predicts that at high frequencies, the cracks will behave as though they are dry, whereas the multiple-set theory predicts that at high frequencies, they will behave as though they are isolated. Unlike [Tod \(2001\)](#), we do not think it strange that in a model involving a single set of cracks, at very low frequencies, the cracks behave as though they are isolated. After all, the wave-induced pressure changes in the fluid inside the cracks will be the same for all cracks if they have the same shape and orientation, suggesting that this behavior is consistent with the (anisotropic Gassmann) relations of [Brown and Korrington \(1975\)](#).

The dry behavior at high frequencies of the cracks in the theory for a single set of communicating cracks is more difficult to understand, but [Hudson et al. \(1996\)](#) and [Tod \(2001\)](#) provided a plausible explanation for this (negative velocity dispersion) (see also [Chakraborty, 2008](#)). Because the cracks are identical (same orientation and aspect ratio), the pressure gradient that drives fluid flow from one crack to another varies on the scale of a wavelength, inversely proportionally to the frequency ω . On the other hand, the diffusion length (defined by [Hudson et al., 1996](#)) varies as $\omega^{-1/2}$. Thus, the diffusion becomes more effective as the frequency tends toward infinity, with the opposite effect as $\omega \rightarrow 0$.

[Tod \(2001\)](#) found that the cracks within a system of nearly aligned cracks behave in a manner consistent with the Brown-Korrington relation at low frequencies, and as though they are isolated with respect to wave-induced fluid flow at high frequencies. This implies that the effective properties predicted by the theories of [Hudson et al. \(1996\)](#) and [Tod \(2001\)](#) will change in a highly discontinuous manner when going from an identical system to a nearly identical system of communicating cracks (through a small perturbation in the parameters of the cracks).

Below, we hope to clarify all these issues addressed by [Tod \(2001\)](#) and to present a more general model of cracked porous media based

on the T-matrix approach (discussed above). [Tod's](#) papers in general and [Tod \(2001\)](#) in particular are very well written and contain many interesting technical details. However, in our opinion, [Tod \(2001\)](#) is slightly confusing because it gives the (wrong) impression that [Hudson et al.'s \(1996\)](#) theory of identical cracks is wrong and that their theory of nonidentical cracks is correct.

Outline

The outline of this paper is as follows. Next, in the “Effective stiffnesses and fluid-pressure polarizations” section, we will discuss how to estimate the effective stiffness tensor of a cracked porous medium in terms of the so-called fluid-pressure-polarization tensors (which determine the wave-induced fluid pressure within each set of cavities) for the different sets of cavities (pores and cracks). In the “Fluid-mass conservation and wave-induced effects” section, we present the evolutionary law for the total fluid-mass concentration within the RVE, and we discuss the difference between stressed and unstressed porosity (for the different sets of cavities). That section contains only well known results, but the formulas are required to make the paper readable and the topic of fluid-mass conservation is highly central in this study.

The “Modified coupling between global flow and squirt flow” section contains new formulas and is the main contribution of this paper. First, we argue that the ansatz used by [Hudson et al. \(1996\)](#), [Tod \(2001\)](#), and [Jakobsen et al. \(2003b\)](#) for the mass flow out of a particular cavity set is inconsistent with the evolutionary law for the total fluid-mass concentration discussed earlier. Then, we show how to modify that ansatz to eliminate the inconsistency.

In the “Modified fluid-pressure-polarization tensors” section, we essentially repeat [Jakobsen et al.'s \(2003b\)](#) calculation, but use a more correct ansatz for the coupling between the global-flow and squirt-flow processes that is consistent with the principle of fluid-mass conservation. When the fluid-pressure-polarization tensors are known, so are the so-called t-matrices and the effective (frequency-dependent and complex-valued) stiffness tensors.

In the “The special case of a single set of cavities” section, we show that the new unified theory of global flow and squirt flow in cracked porous media that is developed in this paper is consistent with the special theory of global flow in models involving only a single set of cavities (developed in Appendix A). In contrast to the relationship between the theories for identical and nonidentical cracks developed by [Hudson et al. \(1996\)](#), [Pointer et al. \(2000\)](#), and [Tod \(2001\)](#). In the “Numerical results and discussion” section, we illustrate many of the problems referred to above and discuss the effects of microstructure on the relative importance of global flow and squirt flow in cracked porous media.

EFFECTIVE STIFFNESSES AND FLUID-PRESSURE POLARIZATIONS

We consider a solid that contains a population of cavities having a distribution of shapes and orientations. The population of cavities is divided into families of inclusions having the same shape and orientation, t-matrix $\mathbf{t}^{(n)}$ (defined below), and (unstressed) porosity $\phi^{(n)}$, labeled by $n = 1, \dots, N$. The effective stiffness tensor \mathbf{C}^* is given by ([Jakobsen et al., 2003a](#); [Jakobsen and Hudson, 2003](#))

$$\mathbf{C}^* = \mathbf{C}^{(0)} + \mathbf{C}_1 : (\mathbf{I}_4 + \mathbf{C}_1^{-1} : \mathbf{C}_2)^{-1}, \quad (1)$$

$$\mathbf{C}_1 = \sum_{r=1}^N \phi^{(r)} \mathbf{t}^{(r)}, \quad (2)$$

and

$$\mathbf{C}_2 = \sum_{r=1}^N \sum_{s=1}^N \phi^{(r)} \mathbf{t}^{(r)} : \mathbf{G}_d^{(rs)} : \mathbf{t}^{(s)} \phi^{(s)}, \quad (3)$$

where $:$ denotes the double scalar product (Auld, 1990). Here, $\mathbf{C}^{(0)}$ is the stiffness tensor for a homogeneous reference medium that can be selected arbitrarily but here is taken to be the stiffness tensor of the solid-matrix material; \mathbf{I}_4 is the (symmetrical) identity for fourth-rank tensors; and $\mathbf{G}_d^{(rs)}$ is given by the strain Green's function (for a material with properties given by $\mathbf{C}^{(0)}$) integrated over a characteristic ellipsoid having the same aspect ratio as $p^{(sr)}(\mathbf{x} - \mathbf{x}')$, which in turn gives the probability density for finding an inclusion of type s at point \mathbf{x}' , given that there is an inclusion of type r at point \mathbf{x} . Ponte Castaneda and Willis (1995) illustrated the fact that the aspect ratio(s) of the correlation function(s) can be selected independently of the aspect ratio(s) that describe the cavities' (ellipsoidal) shapes.

The t-matrix³ for a dry cavity of type n is given by

$$\mathbf{t}_d^{(n)} = -\mathbf{C}^{(0)} : (\mathbf{I}_4 + \mathbf{G}^{(n)} : \mathbf{C}^{(0)})^{-1}, \quad (4)$$

where $\mathbf{G}^{(n)}$ is a fourth-rank tensor (dependent only on $\mathbf{C}^{(0)}$ and the shape and orientation of the n th inclusion type) that can be calculated by using the formulas given in Appendix B for the special case of fully aligned spheroids. The t-matrix for a single cavity of type n that is fully saturated with a homogeneous fluid is given by (Jakobsen et al., 2003b)

$$\mathbf{t}^{(n)} = \mathbf{t}_d^{(n)} + \mathbf{t}_d^{(n)} : \mathbf{S}^{(0)} : (\mathbf{I}_2 \otimes \boldsymbol{\Psi}^{(n)}) : \mathbf{C}^{(0)}, \quad (5)$$

where $\mathbf{S}^{(0)} = (\mathbf{C}^{(0)})^{-1}$ is the compliance tensor of the homogeneous reference medium; \mathbf{I}_2 is the identity for second-rank tensors; \otimes denotes the dyadic tensor product (Jakobsen et al., 2003b); and $\boldsymbol{\Psi}^{(n)}$ is a second-rank tensor that relates the fluid pressure $p_f^{(n)}$ in the n th cavity set to the applied stress $\boldsymbol{\sigma}^{(0)}$ by $p_f^{(n)} = \boldsymbol{\Psi}^{(n)} : \boldsymbol{\sigma}^{(0)}$. After modifying the fluid-dynamic considerations of Jakobsen et al. (2003b), we will evaluate the fluid-pressure-polarization tensor $\boldsymbol{\Psi}^{(n)}$ for the case of a communicating cavity, i.e., a single cavity that is fully saturated with a homogeneous fluid but that can exchange fluid mass with other cavities because of global and/or local pressure gradients associated with passage of a long viscoelastic wave (Figure 1).

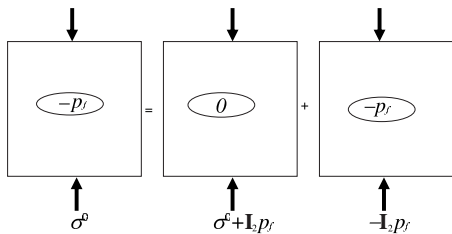


Figure 2. Stress decomposition by linear superposition of small deformations.

³Following Jakobsen et al. (2003a, 2003b), we try to be consistent in the spelling of t-matrix and T-matrix. Uppercase T is associated with overall properties and lowercase t is associated with inclusion properties.

FLUID-MASS CONSERVATION AND WAVE-INDUCED EFFECTS

To evaluate the fluid-pressure-polarization tensor $\boldsymbol{\Psi}^{(n)}$ in the case of a communicating cavity, we will follow Jakobsen et al. (2003b) in using a combination of fluid-dynamic and micromechanical considerations, but will ensure that the total fluid-mass concentration m_f within a representative volume element of the cracked porous medium is conserved. If $\tilde{\phi}^{(n)}$ and $\rho_f^{(n)}$ are the (stressed) porosity and density, respectively, of the n th cavity set, m_f is given by

$$m_f = \sum_{r=1}^N m_f^{(r)}, \quad (6)$$

where

$$m_f^{(n)} = \tilde{\phi}^{(n)} \rho_f^{(n)} \quad (7)$$

is the mass of the fluid inside the cavities of type n within the RVE. Following Hudson et al. (1996) and Jakobsen et al. (2003b), we obtain a differential equation for the time evolution of the total fluid-mass concentration m_f by combining the continuity equation (for fluid-mass conservation) with Darcy's law (for wave-induced fluid flow at the scale of the wavelength):

$$\frac{\partial m_f}{\partial t} = \nabla \cdot \left(\frac{\rho_f}{\eta_f} \boldsymbol{\Gamma} \cdot \nabla p_f \right), \quad (8)$$

where p_f is the average fluid pressure (within the RVE), ρ_f is the average fluid-mass density, η_f is the fluid viscosity, and $\boldsymbol{\Gamma}$ is the (anisotropic) effective-permeability tensor of the cracked porous medium (Jakobsen, 2007). The pressure and density of the fluid inside the n th cavity set are related by (Hudson et al., 1996; Jakobsen et al., 2003b):

$$\frac{\rho_0}{\rho_f^{(n)}} = 1 - \frac{p_f^{(n)}}{\kappa_f}, \quad (9)$$

where ρ_0 is the density of the unstressed fluid and κ_f is the fluid bulk modulus. A similar relation holds between average fluid pressure p_f and density ρ_f .

If a quasistatic (wave-induced) stress field is imposed on a representative volume element of a cracked porous medium, the fluid pressure of the n th cavity set will change because of both fluid flow and porosity change. By using the linear (small-deformation) superposition principle illustrated in Figure 2, Jakobsen et al. (2003a) derived the following first-order expression for the (wave-induced) change in porosity:

$$\frac{\tilde{\phi}^{(n)} - \phi^{(n)}}{\phi^{(n)}} = \mathbf{I}_2 : \mathbf{K}_d^{(n)} : (\boldsymbol{\sigma}^{(0)} + \mathbf{I}_2 p_f^{(n)}) - \mathbf{I}_2 : \mathbf{S}^{(0)} : \mathbf{I}_2 p_f^{(n)}, \quad (10)$$

where

$$\mathbf{K}_d^{(n)} = (\mathbf{I}_4 + \mathbf{G}^{(n)} : \mathbf{C}^{(0)})^{-1} : \mathbf{S}^{(0)} \quad (11)$$

is a fourth-rank tensor that gives us the strain in dry cavities of type n if multiplied by the applied stress from the right.

MODIFIED COUPLING BETWEEN GLOBAL FLOW AND SQUIRT FLOW

In their study of the general case with nondilute concentrations of communicating ellipsoidal cavities having any orientation and aspect ratio(s), [Jakobsen et al. \(2003b\)](#) assumed that the mass flow out of the n th cavity set was given by

$$\frac{\partial m_f^{(n)}}{\partial t} = -\frac{\rho_0 \phi^{(n)}}{\kappa_f \tau} (p_f^{(n)} - p_f), \quad n = 1, \dots, N, \quad (12)$$

where τ is a relaxation parameter of local pressure relaxation or squirt flow ([Jakobsen et al., 2003b](#); [Agersborg et al., 2007](#)). The ansatz 12 is similar to the ansatz used by [Hudson et al. \(1996\)](#) in their studies of the special case with dilute concentrations of cracks having any orientation but a very small aspect ratio (no storage porosity). Also, [Tod \(2001\)](#) used a similar ansatz in his attempt to clarify some of the issues discussed in this paper that are related to the [Hudson et al. \(1996\)](#) models for fully aligned and nonaligned cracks being inconsistent with each other. Hereafter, we refer to equation 12 as “old ansatz 12.”

The coupling between the processes of global flow and squirt flow implied by old ansatz 12 is inconsistent with the principle of fluid-mass conservation. Consider the simple case of a model structure involving a single set of cavities. Because this special case corresponds with $N = 1$, the mean pressure p_f now equals pressure $p_f^{(1)}$ in the fluid inside the only set of cavities, so that the mass flow out of the cavities always is zero (according to old ansatz 12). Because $\rho_f^{(1)} \phi^{(1)}$ also equals the total fluid mass m_f (defined in equation 6), old ansatz 12 implies that the change in the total fluid-mass concentration is zero, whereas evolution law equation 8 predicts that pressure gradients at the scale of the wavelength should lead to a nonzero change in the total fluid-mass concentration. In other words, old ansatz 12 is not consistent with evolution law equation 8.

Old ansatz 12 predicts that there will be no global flow in models involving a single set of fully aligned cracks (with no local pressure gradients and consequently no squirt flow). This means that wave-induced fluid flow is not possible at any scale in models involving only a single cavity set (according to old ansatz 12). Clearly, this behavior is in contrast with common sense, as well as with [Hudson et al.’s \(1996\)](#) special theories of global flow in models involving fully aligned cracks and with the models developed in Appendix A that involve fully aligned ellipsoidal cavities.

Old ansatz 12 implies that

$$\frac{\partial \hat{m}^{(m)}}{\partial t} - \frac{\partial \hat{m}^{(n)}}{\partial t} = -\frac{\rho_0}{\kappa_f \tau} (p_f^{(m)} - p_f^{(n)}), \quad (13)$$

where the normalized mass densities $\hat{m}^{(r)}$ are defined by

$$\hat{m}^{(r)} = m_f^{(r)} / \phi^{(r)}, \quad r = 1, \dots, N \quad (14)$$

and N still is arbitrary. Equation 13 describes the exchange of fluid mass between two cavities within a representative volume element of the cracked porous medium, much like in the [Chapman et al. \(2002\)](#) network model. Hereafter, we therefore refer to equation 13 as the “network-ansatz.” Note that network ansatz 13 does not imply that old ansatz 12 is true. In other words, old ansatz 12 contains an error (related to global flow) that disappears when old ansatz 12 is used to study the exchange of fluid mass between two cavity types within a representative volume element.

To transform network ansatz 13 into an equivalent form (a “new” ansatz) that also involves the average fluid pressure p_f , we first write it more explicitly as

$$\begin{aligned} \frac{\partial \hat{m}^{(1)}}{\partial t} - \frac{\partial \hat{m}^{(1)}}{\partial t} &= -\frac{\rho_0}{\kappa_f \tau} (p_f^{(1)} - p_f^{(1)}), \\ \frac{\partial \hat{m}^{(1)}}{\partial t} - \frac{\partial \hat{m}^{(N)}}{\partial t} &= -\frac{\rho_0}{\kappa_f \tau} (p_f^{(1)} - p_f^{(N)}). \end{aligned} \quad (15)$$

In the above array of N different equations, we multiply the equation labeled with $r = 1, \dots, N$ by $\phi^{(r)}$, sum the N different resultant equations, and use the definition of the total fluid mass m_f in equation 6. This gives

$$\frac{\partial m_f^{(1)}}{\partial t} - \frac{\phi^{(1)}}{\phi} \frac{\partial m_f}{\partial t} = -\frac{\rho_0 \phi_0^{(1)}}{\kappa_f \tau} (p_f^{(1)} - p_f), \quad (16)$$

where we have related the total porosity ϕ to the average fluid pressure p_f by

$$\phi p_f \equiv \sum_{r=1}^N \phi^{(r)} p_f^{(r)}, \quad (17)$$

suggesting that the (artificial) weight functions discussed in [Tod’s \(2001\)](#) Appendix A no longer are needed. Because the labeling of different cavities is arbitrary, it must be generally true that

$$\frac{\partial m_f^{(n)}}{\partial t} - \frac{\phi^{(n)}}{\phi} \frac{\partial m_f}{\partial t} = -\frac{\rho_0 \phi_0^{(n)}}{\kappa_f \tau} (p_f^{(n)} - p_f), \quad n = 1, \dots, N. \quad (18)$$

The fluid-mass flow out of the n th cavity set now is corrected for the fraction of the change in the total fluid-mass concentration for which it is responsible (through the second term on the left side of equation 18). Therefore, we believe that “new ansatz” 18 makes more physical sense than old ansatz 12.

To verify this, we again consider the special case of a single cavity. Because $N = 1$ for this special case, we now get zero on the left and right sides (according to new ansatz 18), suggesting that new ansatz 18 (unlike old ansatz 12) does not prohibit global flow in models in which there is no squirt flow (because of lack of local pressure gradients). Physically, because the two terms on the left side are equal (when $N = 1$), the decrease per unit time in the fluid mass inside the first and only set of cavities within the RVE (Figure 1) equals the total fluid mass that flows out of the RVE per unit time. In other words, there is global flow but no squirt flow (in the new model only) when $N = 1$. Below we explore the effects that the modifications we made to old ansatz 12 have on the polarization tensors and the corresponding t-matrices, stiffnesses, and anelastic wave-characteristics of models involving single and multiple sets of communicating cavities (at finite concentration).

MODIFIED FLUID-PRESSURE-POLARIZATION TENSORS

Following [Jakobsen et al. \(2003b\)](#), we now introduce a second-rank tensor Ψ that relates the applied stress $\boldsymbol{\sigma}^{(0)}$ to the average fluid pressure p_f using $p_f = \Psi : \boldsymbol{\sigma}^{(0)}$. By working toward first order in the small quantities $p_f^{(n)} / \kappa_f$ and $(\tilde{\phi}^{(n)} - \phi^{(n)}) / \phi^{(n)}$ and by assuming that

the propagating-plane harmonic wave has angular frequency ω and wave vector \mathbf{k} (see equation B-11), we get

$$\boldsymbol{\psi}^{(n)} = \frac{(1 - \Delta)\boldsymbol{\psi} - i\omega\tau\kappa_f\mathbf{I}_2:\mathbf{K}_d^{(n)}}{1 + i\omega\gamma^{(n)}\tau} \quad (19)$$

and

$$\gamma^{(n)} = 1 + \kappa_f\mathbf{I}_2:(\mathbf{K}^{(n)} - \mathbf{S}^{(0)}):\mathbf{I}_2, \quad (20)$$

where

$$\Delta \equiv \frac{\kappa_f\tau}{\phi\eta_f}\Gamma_{ij}k_i k_j \quad (21)$$

is a new term related to the coupling introduced in equation 18 between the processes of global flow and squirt flow.

To find the $\boldsymbol{\psi}$ tensor for substitution into equation 19, we first derive an expression for m_f combining equations 9 and 10. The resultant expression for m_f is inserted into a Fourier representation of the evolution law, equation 8. It follows that

$$\boldsymbol{\psi} = -\Theta \sum_{r=1}^N \frac{\phi^{(r)}\mathbf{I}_2:\mathbf{K}_d^{(r)}}{1 + i\gamma^{(r)}\tau}, \quad (22)$$

where

$$\Theta = \kappa_f \left[\sum_{r=1}^N \frac{\phi^{(r)}\gamma^{(r)}}{1 + i\omega\gamma^{(r)}\tau} (1 - \Delta) - \frac{i\kappa_f\Gamma_{ij}k_i k_j}{\eta_f\omega} \right]^{-1}. \quad (23)$$

It follows from equations 19, 22, and 23 that

$$\boldsymbol{\psi}^{(n)} = -\frac{\tilde{\Theta} \sum_r \frac{\phi^{(r)}\mathbf{I}_2:\mathbf{K}_d^{(r)}}{1 + i\omega\gamma^{(r)}\tau} + i\omega\tau\kappa_f\mathbf{I}_2:\mathbf{K}_d^{(n)}}{1 + i\omega\gamma^{(n)}\tau}, \quad (24)$$

where

$$\tilde{\Theta} \equiv \Theta(1 - \Delta) = \kappa_f \left[\sum_{r=1}^N \frac{\phi^{(r)}\gamma^{(r)}}{1 + i\omega\gamma^{(r)}\tau} + \frac{i\kappa_f\Gamma_{ij}k_i k_j}{\eta_f\omega(1 - \Delta)} \right]^{-1}. \quad (25)$$

Only if $\Delta \leq 1$ does the expression for the cavity-fluid-pressure-polarization tensor represented by formulas 24 and 25 degenerate to the one derived by Jakobsen et al. (2003b) in connection with their generalization of the theory for interconnected nonaligned cracks developed by Hudson et al. (1996) and Tod (2001). Inserting formula 24 for $\boldsymbol{\psi}^{(n)}$ into expression 5 for the t-matrix of a communicating cavity yields the same expressions as in Jakobsen et al. (2003b), but with a modified Θ term, denoted by $\tilde{\Theta}$.

THE SPECIAL CASE OF A SINGLE SET OF CAVITIES

In the special case of a single set of cavities, when $N = 1$, the average pressure p_f is equal to pressure $p_f^{(1)}$ in the fluid inside the first and only cavity set, so that

$$\boldsymbol{\psi}^{(n)}|_{n=N=1} = \boldsymbol{\psi}|_{N=1} \equiv \boldsymbol{\psi}_s. \quad (26)$$

Equation 26 follows directly from the definition of average fluid pressure p_f in equation 17, but we also have verified this by using equations 22–25.

From the definition of $\boldsymbol{\psi}$ in equation 22, we get

$$\boldsymbol{\psi}_s = -\Theta_s \frac{\phi^{(1)}\mathbf{I}_2:\mathbf{K}_d^{(1)}}{1 + i\omega\gamma^{(1)}\tau}, \quad (27)$$

where

$$\Theta_s = \kappa_f \left[\frac{\phi^{(1)}\gamma^{(1)}}{1 + i\omega\gamma^{(1)}\tau} (1 - \Delta) + \frac{i\kappa_f\Gamma_{ij}k_i k_j}{\eta_f\omega} \right]. \quad (28)$$

By using the definition of Δ in equation 21, we can rewrite equations 27 and 28 exactly as

$$\boldsymbol{\psi}_s = \kappa_f \left(\phi^{(1)}\gamma^{(1)} - \frac{ik_i k_j \Gamma_{ij} \kappa_f}{\eta_f \omega} \right)^{-1} \phi^{(1)}\mathbf{I}_2:\mathbf{K}_d^{(1)}. \quad (29)$$

This equation is identical to equation A-14 in Appendix A, which was obtained using a procedure that ignores squirt flow. In other words, the unified theory of global flow and squirt flow developed in this paper (for models involving an arbitrary number of cavity sets) is consistent with the special theory of global flow derived in Appendix A (for models involving a only single set of cavities).

This is in contrast to the relationship between the theories of identical nonidentical cracks developed by Hudson et al. (1996), Pointer et al. (2000), and Tod (2001). In the case of a single set of cavities (characterized by the same shape and orientation), all cracks will have the same wave-induced change in fluid pressure, so that there are no local pressure gradients and consequently there is no squirt flow. Therefore, it is not surprising that the expression for p_f in equation 29 does not contain the characteristic time τ for squirt flow. If the original version of the T-matrix approach developed by Jakobsen et al. (2003b), which is a generalization of Hudson et al.'s (1996) theory for nonaligned communicating cracks, is applied to the special case when $N = 1$, the τ parameter will not disappear from the resultant equation for p_f ; therefore, for many reasons we believe that the modifications we have made to the coupling between the processes of global flow and squirt flow that is caused by fluid-mass conservation make good physical sense.

NUMERICAL EXPERIMENTS

The next step is to perform numerical experiments to investigate the effects of microstructure on the relative importance of global flow and squirt flow in idealized models for cracked porous media. But first we need to discuss how to obtain real-valued phase velocities and attenuation spectra from the frequency-dependent and complex-valued effective stiffness tensor \mathbf{C}^* . In general, \mathbf{C}^* depends on wave vector \mathbf{k} and angular frequency ω ; however, following Hudson et al. (1996), Pointer et al. (2000), Tod (2001), Jakobsen et al. (2003b), and Jakobsen and Hudson (2003), we eliminate the dependency of \mathbf{C}^* on the (effective) wave vector \mathbf{k} by using the approximation $k \approx \omega/V^{(0)}$, where $V^{(0)}$ is the speed of the wave mode under consideration in the solid matrix and k is the length of \mathbf{k} . We then calculate the frequency-dependent and complex-valued phase velocity V in the direction $\hat{\mathbf{k}} = \mathbf{k}/k$ of wave propagation by inserting \mathbf{C}^* into the well known Christoffel equation (Auld, 1990), which can be solved by using the eigenvectors/eigenvalues method (Jakobsen et al.,

2003b; Carcione, 2007). Real-valued phase velocities and attenuation (inverse-quality) factors then can be obtained from

$$\mathbf{V}_p = \left[\text{Re} \left(\frac{1}{V} \right) \right]^{-1} \hat{\mathbf{k}} \quad (30)$$

and

$$Q = \frac{\text{Re}(V^2)}{\text{Im}(V^2)}, \quad (31)$$

as discussed by Carcione (2007).

Figure 3 shows the velocity and the attenuation spectra we estimated for the special case of a solid that contains a single set of fully aligned, low-aspect-ratio, spheroidal cracks. The solid curves and the dashed and dotted curves represent the predictions of the new and old versions of the T-matrix approach, respectively. The new theory predicts that the velocity dispersion will always be nonpositive, like in Hudson et al.'s (1996) model of identical communicating cracks. The velocity and the attenuation spectra of the old theory (but not of the new one) depend on the characteristic time for squirt flow τ . Because local pressure gradients do not exist in this model, dependency on τ (in the old version of the T-matrix approach) does not make good physical sense. Interestingly, the old and new theories predict a negative velocity dispersion.

The main difference between the old and new theories is in the behavior in the limit of very high frequencies. The old theory predicts that in this model, at high frequencies cracks will behave as though they are isolated with respect to fluid flow, whereas the new theory predicts that when the frequency approaches infinity, they will be-

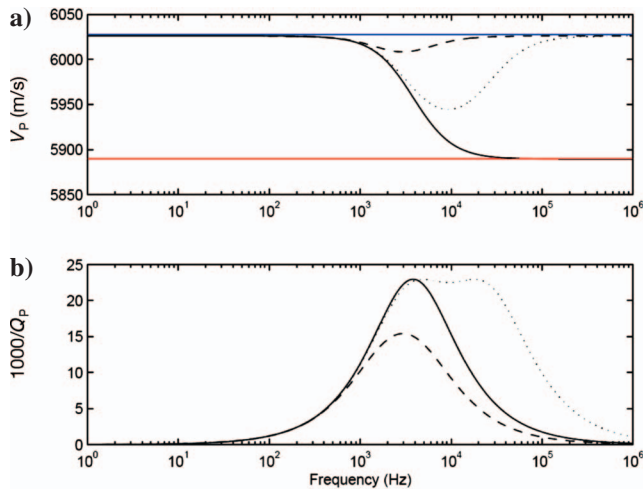


Figure 3. The case of fully aligned cracks revisited: Comparison of new (solid curve) and old (dashed and dotted curves) T-matrix estimates of the velocity and attenuation spectra of a plane wave propagating normal to the cracks in a model with a single set of identical (spheroidal) cracks that are characterized by a 0.005 aspect ratio and a 0.01 crack density. The cracked medium was assumed to be fully saturated with a single fluid (water), and the permeability was 1 darcy ($9.868233 \times 10^{-13} \text{ m}^2$). The solid and dashed curves correspond to $\tau = 10^{-5} \text{ s}$ and the dotted curves correspond to $\tau = 10^{-6} \text{ s}$. The solid matrix was characterized by the bulk modulus $\kappa = 37 \text{ MPa}$, the shear modulus $\mu = 44 \text{ MPa}$, and the density $\rho = 2500 \text{ kg/m}^3$. The red and upper blue horizontal lines/curves in (a) correspond to cracks that are fully drained (dry) and completely isolated with respect to wave-induced fluid flow, respectively.

have as though they are completely drained (dry). As discussed in the “Introduction,” the new theory’s prediction of dry behavior at very high frequencies is consistent with Hudson et al.’s (1996) theory for fully aligned communicating cracks, and it makes good physical sense.

At the same time, we note that a negative velocity dispersion is not commonly observed, although Chakraborty (2008) was motivated by observations of negative velocity dispersion in nongeologic media. As we show below, the reason for this could be that local pressure gradients and therefore squirt-flow effects are always present to some degree in real rocks (Klimentos and McCann, 1988) because real rocks always contain more than one set of cavities. Another possibility is that the global-flow part of the present theory is incomplete, or that the predictions will change if we include the nonlocal effects associated with the effective stiffness tensor being a function of effective wave vector \mathbf{k} as well as of angular frequency ω . An investigation of this topic, in conjunction with a test of consistency with the Kramers-Kronig relations and nonnegative work criterion from the theory of viscoelastic waves (Carcione, 2007) will be reported in a subsequent paper.

Figure 4 is associated with two sets of cavities that are characterized by the same orientation but aspect ratios that might not be equal. Figure 4a and b compares results obtained by using identical aspect ratios (solid curves) and nearly identical aspect ratios (dashed curves) for the two sets of cavities. Figure 4c and d represents results obtained by using very different aspect ratios (a mixture of spherical pores and aligned cracks). As expected, we see that the introduction of local pressure gradients (by perturbation in the aspect ratios) leads to squirt flow in addition to global flow. Clearly, small perturbations in the aspect ratios lead to small changes in velocity and the attenuation spectra. A comparison of Figure 4a and b with Figure 4c and d suggests that the effect of introducing larger and larger aspect-ratio

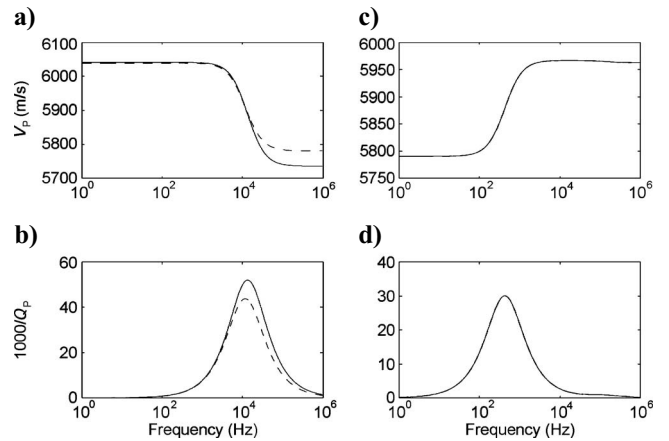


Figure 4. The effects of cavity aspect ratio: a comparison of new T-matrix estimates of the velocity and attenuation spectra of a plane wave propagating normal to the cavities in a model with two sets of cavities that are characterized by the same orientation but aspect ratios that might not be equal. Panels (a) and (b) show results obtained by assuming identical aspect ratios ($\alpha^{(1)} = \alpha^{(2)} = 0.001$; solid curves) and nearly identical aspect ratios ($\alpha^{(1)} = 0.001$, $\alpha^{(2)} = 0.002$; dashed curves). Panels (c) and (d) show results obtained by using very different aspect ratios for the two cavity sets: ($\alpha^{(1)} = 0.001$, $\alpha^{(2)} = 1$). The properties of the solid matrix are the same as in Figure 3, but the permeability and characteristic time for squirt flow here were taken to be 500 mD and 10^{-5} s , respectively. The crack density for sets 1 and 2 was 0.1 and 0.005, respectively.

differences is to move from a global-flow-dominated system to a squirt-flow-dominated system.

Figure 5 illustrates more or less the same effects as Figure 4, but for a constant aspect ratio of the cracks and varied crack orientations (We used the orientation-averaging method of Jakobsen et al. [2003b], summarized in Appendix C). Figure 5a and b compares results obtained for fully aligned cracks (solid curves) and nearly aligned cracks (dashed curves), whereas Figure 5c and d shows results obtained for randomly oriented cracks. The main point here is that a small perturbation in the orientation of the cracks leads to squirt-flow (in addition to global-flow) effects, but these effects will be small unless the perturbations are large.

It is interesting that the attenuation spectra for the model of randomly oriented cracks (Figure 5c and d) have two attenuation peaks, corresponding to squirt flow (at relatively low frequencies) and global flow (at relatively high frequencies). Similar plots have been made for other values of the permeability and squirt-flow constants. We have seen that increasing the permeability (or fluid mobility) moves the attenuation peak associated with global flow to the left, whereas decreasing the squirt-flow constant τ and/or the γ constant(s) moves the attenuation peak associated with squirt flow to the right. In other words, global flow and squirt flow might dominate within a particular frequency range, depending on a range of constants. We have found that as the crack system changes from fully aligned to randomly oriented (the standard deviation of the crack orientation-distribution function changes from zero to infinity), there is

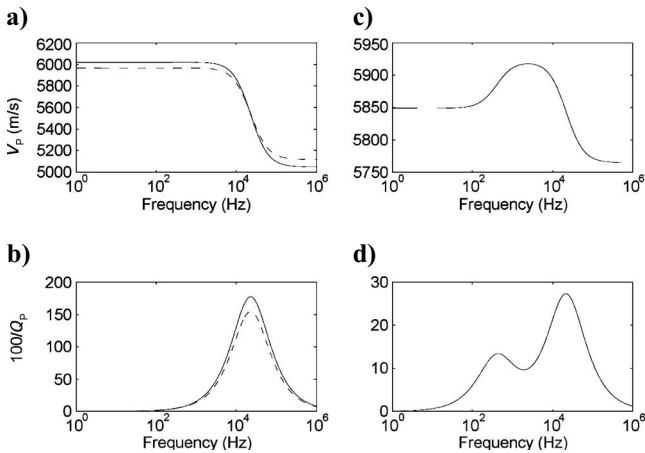


Figure 5. The effects of crack orientation: a comparison of new T-matrix estimates of the velocity and attenuation spectra of a plane wave propagating along the symmetry axis of a transversely isotropic medium with a vertical symmetry axis (along the x_3 -axis) composed of cracks that are characterized by the same aspect ratio ($\alpha = 0.005$), but not necessarily by the same orientation. Following Jakobsen et al. (2003b), here we used a Gaussian orientation-distribution function, characterized by standard deviation σ . Panels (a) and (b) show results obtained by assuming fully aligned cracks ($\sigma = 0$) and nearly aligned cracks ($\sigma = \pi/16$), respectively. Panels (c) and (d) show results for the extreme case of randomly oriented cracks ($\sigma = \infty$). The properties of the solid matrix and the characteristic time for squirt flow are the same as in Figure 3, but the permeability was 1 darcy ($9.868233 \times 10^{-13} \text{ m}^2$). The aspect ratio of the cracks was 0.001.

a continuous change in the behavior of a cracked solid from completely global-flow-dominated to more squirt-flow-dominated. The results in Figure 5 are in stark contrast to the relationship between the fully aligned and partially aligned crack models discussed by Hudson et al. (1996) and Tod (2001), but they make much more physical sense.

DISCUSSION

The associate editor suggested that even when all the cavities have the same shape and orientation, squirt flow might occur because cavity interaction effects (stress propagation through the solid matrix material) could lead to local pressure gradients (different deformations of different cavities). This is true, of course, but not relevant for our analysis because t-matrix for a communicating cavity is related to the response of a single (fully saturated) cavity that by definition is isolated with respect to stress propagation through the solid matrix but can exchange fluid mass with other cavities because of local and/or global pressure gradients associated with the passage of a long acoustic or viscoelastic wave.

The T-matrix approach we used to estimate the effective stiffness values (consistent with Hudson et al.'s (1996) second-order correction and Eshelby's (1957) noninteracting-cavity model) includes the effects of cavity-cavity interaction through the use of two-point correlation functions of ellipsoidal symmetry. However, all these cavity-interaction effects are decomposed into products of pairs of t-matrices and constant tensors (given by suitable integrals of the modified strain Green tensor functions associated with the solid matrix material). In other words, we include some of these cavity-interaction effects in our calculations of the effective stiffness tensor, but not in our evaluation of the t-matrix for a single communicating cavity.

Jakobsen (2004) developed an interacting inclusion model of wave-induced fluid flow that could be combined with the cavity fluid-pressure-polarization results derived in this study to try to develop a unified theory of global flow and squirt flow in cracked porous media that also includes the (higher-order) interaction effects described by the associate editor. However, incorporating such interacting effects (which become extremely small in the case of dilute cavity concentrations when the first-order stiffness-based approximation is valid) is far beyond the scope of the present study.

In any case, we now have stopped a serious error (related to fluid-mass conservation) from propagating from Hudson et al. (1996) through Pointer et al. (2000), Tod (2001), and Jakobsen et al. (2003b) and into the wider geophysical literature.⁴ Because the (revised and more correct) unified theory of global flow and squirt flow developed in this paper differs from the one developed by Jakobsen et al. (2003b) only by a term (ensuring consistency with the principle of fluid-mass conservation) that goes to zero in the limit of zero frequency, earlier demonstrations of consistency with the (anisotropic Gassmann) relations of Brown and Korringa (1975) provided by Jakobsen et al. (2003b) and Jakobsen (2004) remain valid. Our analysis and numerical results suggest that global flow is far more important than we have previously believed and that numerical experiments and attempts at analyzing experimental data (e.g., Tod and Liu, 2002) that are based on the work of Hudson et al. (1996), Tod (2001), Jakobsen et al. (2003b), and Jakobsen and Hudson (2003)

⁴At the time of this writing, the theory of Hudson et al. (1996) had been cited in 80 papers (according to the Institute for Scientific Information [ISI] Web of Science).

might be partially incorrect. By partially, we mean that the correction term we have introduced in this paper becomes negligible when the permeability (or mobility) is very small; which is the case for many carbonate rocks (Agersborg et al., 2008), but is in contrast to the study of Tod and Liu (2002), which involved rocks with relatively high fluid mobilities.

If the unified model is applied to the special case of a model involving a single set of cavities (characterized by the same orientation and shape), the results become identical with those obtained by using a special theory of global flow (developed in Appendix A, using a method that ignores squirt flow). This is in contrast with the relationship that exists between the theories of identical and nonidentical cracks that Hudson et al. (1996), Pointer et al. (2000), and Tod (2001) developed. However, we still are unsure that this paper will be the last word in the discussion about the relative importance of global flow and squirt flow (which depends on the microstructure). It is possible that the method we used to develop the special theory of global flow in models involving a single set of cavities is incomplete or is based on approximations that become less accurate at higher frequencies (smaller wavelengths, larger global pressure gradients). After all, wave vector \mathbf{k} entered the formula for the effective stiffness tensor through a linearization of the evolution law for the total fluid-mass concentration m_f , and the global pressure gradient was taken to be $-\mathbf{i}\mathbf{k}$ (after a 4D Fourier transformation).

It also is possible that different numerical results would have been obtained had we not followed Hudson et al. (1996), Pointer et al. (2000), and Tod (2001) in ignoring nonlocal effects associated with the dependence of effective stiffness tensor \mathbf{C}^* on effective wave-number \mathbf{k} (as well as on angular frequency ω) rather than on the reference (unperturbed) wave vector $k^{(0)}$ associated with the solid matrix. Note that Chakraborty (2008) (during the time of this writing) predicted negative velocity dispersion by a nonlocal poroelastic theory. Jakobsen currently is preparing a related paper that focuses on these nonlocal issues (related to the slow P-wave of Biot, 1962). In any case, we believe that the present paper represents a step forward because the unified theory of global flow and squirt flow in models involving an arbitrary number of cavity sets is consistent with the special theory of global flow in models involving only a single set of cavities.

CONCLUSIONS

We have discovered and removed an inconsistency or error (related to the coupling between the processes of global flow and squirt flow because of conservation of fluid mass) in an existing expression for the frequency-dependent and complex-valued effective stiffness tensors of cracked porous media associated with the T-matrix approach to rock physics (which includes but is more general than the frequently cited theory of communicating nonidentical cracks introduced by Hudson et al. [1996]).

Our analysis and results suggest that the relative importance of global flow and squirt flow depends on the nature and content of the pores and cracks (including the total porosity, the fluid saturation, and the statistical distribution of shapes and orientations), as well as on the fluid mobility and the characteristic time for squirt flow. Therefore, detailed modeling might often be required to analyze the anisotropic velocity and the attenuation spectra of real media.

It appears that in principle, the velocity dispersion of cracked porous media can be negative or positive. However, a negative velocity dispersion always is associated with global flow, and squirt flow

(which tends to produce a positive velocity dispersion) often dominates over global flow unless all cavities are characterized by the same or nearly the same shape and orientation (and/or the fluid mobility is very high). This means that negative velocity dispersion might not be encountered often in practice because real rocks normally are characterized by a wide variety of different pore shapes (and their fluid mobility often is insufficiently high for global flow to dominate over squirt flow). Nevertheless, one should be careful in ignoring the process of global flow because this is coupled with the process of squirt flow. In cases where squirt flow dominates over global flow, the velocity dispersion might be positive, but the numerical values of the predicted (anisotropic) velocity and the attenuation spectra might be affected significantly by global flow (depending on the fluid mobility and microstructure).

ACKNOWLEDGMENTS

We thank Simon Tod for his helpful comments. Morten Jakobsen thanks the British Geological Survey (including the Edinburgh Anisotropy Project leader, X.Y. Li) for providing a stimulating work environment during his sabbatical period, when most of this work was done. We thank the associate editor, Vladimir Grechka, for fruitful discussions.

APPENDIX A

SPECIAL THEORY OF GLOBAL FLOW

This appendix is essentially a generalization of Hudson et al.'s (1996) special theory of global flow for the simple case of a solid that contains a dilute concentration of spheroidal communicating cracks that are characterized by the same (low) aspect ratio and orientation. By generalization, we mean that our special theory of global flow (represented by a combination of the T-matrix approximations discussed in the "Effective stiffnesses and fluid-pressure polarization" section and the expression for the wave-induced change in fluid pressure derived in this appendix) is valid for nondilute concentrations of ellipsoidal cavities that are characterized by arbitrary aspect ratios and orientations.

If a static stress field $\boldsymbol{\sigma}^{(0)}$ is imposed on a representative volume element (containing a large number of communicating cavities that are characterized by the same shape and orientation), the pressure in the fluid changes because of changes in both porosity and fluid flow. In the absence of the fluid, the porosity changes according to

$$\frac{\tilde{\phi} - \phi}{\phi} = \mathbf{I}_2 : \mathbf{K}_d : \boldsymbol{\sigma}^{(0)}, \quad (\text{A-1})$$

where

$$\mathbf{K}_d = (\mathbf{I}_4 + \mathbf{G} : \mathbf{S}^{(0)})^{-1} : \mathbf{S}^{(0)}. \quad (\text{A-2})$$

If fluid is present, we may write

$$\frac{\tilde{\phi} - \phi}{\phi} = \mathbf{I}_2 : \mathbf{K}_d : (\boldsymbol{\sigma}^{(0)} + \mathbf{I}_2 p_f) - \mathbf{I}_2 : \mathbf{S}^{(0)} : \mathbf{I}_2 p_f, \quad (\text{A-3})$$

where p_f is the induced fluid pressure (see Figure 2). Equation A-3 is an application of the linear superposition principle used in Gueguen and Palciauskas (1994) and can be rewritten as

$$\tilde{\phi} = \phi + \phi \mathbf{I}_2 : \mathbf{K}_d : \boldsymbol{\sigma}^{(0)} + \phi \frac{\gamma - 1}{\kappa_f} p_f, \quad (\text{A-4})$$

where

$$\gamma = 1 + \kappa_f \mathbf{I}_2 : (\mathbf{K}_d - \mathbf{S}^{(0)}) : \mathbf{I}_2. \quad (\text{A-5})$$

If the wavelengths are long relative to the scale size of the heterogeneities within the RVE, we may apply the static result to dynamic situations, corresponding to passage of an acoustic wave or a seismic wave. However, the total fluid-mass concentration will change because of global flow, so that fluid pressure p_f will depend on time or frequency (after Fourier transformation). Below we use the above formulas and the evolution law for m_f in equation 8 to find an expression for wave-induced fluid pressure in the frequency domain.

Total fluid-mass concentration m_f is given by

$$m_f = \rho_f \tilde{\phi}. \quad (\text{A-6})$$

From the constitutive relation for the fluid:

$$\frac{\rho_0}{\rho_f} = 1 - \frac{p_f}{\kappa_f} \quad (\text{A-7})$$

and equation A-4, we get

$$m_f = \rho_0 \left(1 + \frac{p_f}{\kappa_f} \right) \left(\phi + \phi \mathbf{I}_2 : \mathbf{K}_d : \boldsymbol{\sigma}^{(0)} + \phi \frac{\gamma - 1}{\kappa_f} p_f \right) \quad (\text{A-8})$$

or

$$m_f = \rho_0 \phi \left(1 + \mathbf{I}_2 : \mathbf{K}_d : \boldsymbol{\sigma}^{(0)} + \frac{\gamma p_f}{\kappa_f} \right) \quad (\text{A-9})$$

to first order in p_f/κ_f .

We now assume that we are dealing with a plane harmonic plane wave, so that the wave-induced change in fluid pressure p_f is given by

$$p_f = p_0 \exp i(\omega t - \mathbf{k} \cdot \mathbf{x}), \quad (\text{A-10})$$

where p_0 is the amplitude, ω is the angular frequency, and \mathbf{k} is the wave (wavenumber) vector. From equations A-9 and A-10, it follows that

$$\frac{\partial m_f}{\partial t} = i\omega \rho_0 \phi \left(\mathbf{I}_2 : \mathbf{K}_d : \boldsymbol{\sigma}^{(0)} + \frac{\gamma p_f}{\kappa_f} \right). \quad (\text{A-11})$$

Also, the evolution law equation 8 implies that

$$\frac{\partial m_f}{\partial t} = \frac{i^2 \rho_0}{\eta_f} \Gamma_{ijk} k_j p_f \quad (\text{A-12})$$

to first order in p_f/κ_f . It follows from the above equations that

$$p_f = \boldsymbol{\psi}_s : \boldsymbol{\sigma}^{(0)}, \quad (\text{A-13})$$

where

$$\boldsymbol{\psi}_s = \kappa_f \left(\phi \gamma - \frac{ik_i k_j \Gamma_{ij} \kappa_f}{\eta_f \omega} \right)^{-1} \phi \mathbf{I}_2 : \mathbf{K}_d. \quad (\text{A-14})$$

By approximating the effective wavenumber k by its unperturbed value ($k^{(0)} = \omega/V$, where V is the wave-speed in the uncracked solid

matrix), it can be shown that $p_f \rightarrow 0$ when $\omega \rightarrow \infty$. Also, one can show analytically and numerically that the low-frequency limit corresponds to cavities that are isolated with respect to wave-induced (global) fluid flow, like in the Hudson et al. (1996) model of fully aligned communicating cracks.

APPENDIX B

EVALUATION OF THE G TENSOR

The tensor $\mathbf{G}^{(r)}$ is given by (Jakobsen and Johansen, 2005)

$$\mathbf{G}^{(r)} = -\mathbf{S}^{(r)} : \mathbf{S}^{(0)}, \quad (\text{B-1})$$

where $\mathbf{S}^{(r)}$ is the Eshelby tensor of the ellipsoid. The Eshelby tensor generally is given in terms of first and second elliptical integrals (Jakobsen et al., 2003a; Jakobsen and Johansen, 2005). In the case an isotropic matrix material containing spheroidal inclusions with semiaxes $a_1^{(r)} = a_2^{(r)} = a_r$ and $a_3^{(r)} = b_r$ and whose symmetry axis is aligned in the x_3 -direction, the elliptical integrals can be evaluated analytically (Jakobsen et al., 2003a). If the matrix material is isotropic then the components of $S_{ijkl}^{(r)}$ are given by (Jakobsen and Johansen, 2005)

$$S_{1111}^{(r)} = S_{2222}^{(r)} = \frac{3}{8(1-\nu)} \frac{\alpha_r^2}{\alpha_r^2 - 1} + \frac{1}{4(1-\nu)} \times \left[1 - 2\nu - \frac{9}{4(\alpha_r^2 - 1)} \right] q,$$

$$S_{3333}^{(r)} = \frac{1}{2(1-\nu)} \left\{ 1 - 2\nu + \frac{3\alpha_r^2 - 1}{\alpha_r^2 - 1} - \left[1 - 2\nu + \frac{3\alpha_r^2}{\alpha_r^2 - 1} \right] q \right\},$$

$$S_{1122}^{(r)} = S_{2211}^{(r)} = \frac{1}{4(1-\nu)} \left\{ \frac{\alpha_r^2}{2(\alpha_r^2 - 1)} - \left[1 - 2\nu + \frac{3}{4(\alpha_r^2 - 1)} \right] q \right\},$$

$$S_{1133}^{(r)} = S_{2233}^{(r)} = \frac{1}{2(1-\nu)} \left\{ \frac{-\alpha_r^2}{\alpha_r^2 - 1} + \frac{1}{2} \left[\frac{3\alpha_r^2}{\alpha_r^2 - 1} - (1 - 2\nu) \right] q \right\},$$

$$S_{3311}^{(r)} = S_{3322}^{(r)} = \frac{1}{2(1-\nu)} \left\{ 2\nu - 1 - \frac{1}{\alpha_r^2 - 1} + \left[1 - 2\nu + \frac{3}{2(\alpha_r^2 - 1)} \right] q \right\},$$

$$\begin{aligned}
S_{1212}^{(r)} &= \frac{1}{4(1-\nu)} \left\{ \frac{\alpha_r^2}{2(\alpha_r^2-1)} \right. \\
&\quad \left. + \left[1 - 2\nu - \frac{3}{4(\alpha_r^2-1)} \right] q \right\}, \\
S_{1313}^{(r)} &= S_{2323}^{(r)} \\
&= \frac{1}{4(1-\nu)} \left\{ 1 - 2\nu - \frac{\alpha_r^2+1}{\alpha_r^2-1} \right. \\
&\quad \left. - \frac{1}{2} \left[1 - 2\nu - \frac{3(\alpha_r^2+1)}{\alpha_r^2-1} \right] q \right\}, \quad (\text{B-2})
\end{aligned}$$

where ν is the Poisson ratio of the matrix, $\alpha_r = b_r/a_r$ is the aspect ratio of the r th spheroid, and q is given by

$$q = \frac{\alpha_r}{(1-\alpha_r^2)^{3/2}} [\cos^{-1}\alpha_r - \alpha_r(1-\alpha_r^2)^{1/2}] \quad (\text{B-3})$$

when $\alpha_r \leq 1$.

From these results, we see that for spheres ($\alpha_r = 1, q = 2/3$),

$$S_{ijkl}^{(r)} = \frac{5\nu-1}{15(1-\nu)} \delta_{ij}\delta_{kl} + \frac{4-5\nu}{15(1-\nu)} (\delta_{ik}\delta_{jl} + \delta_{il}\delta_{jk}). \quad (\text{B-4})$$

If r refers to a typical flat compliant Hudson-crack (characterized by $\alpha_r \rightarrow 0, q \rightarrow 0$), then the only nonvanishing components are

$$\begin{aligned}
S_{3333}^{(r)} &= 1, \\
S_{3311}^{(r)} &= S_{3322}^{(r)} = \frac{\nu}{1-\nu}, \\
S_{1313}^{(r)} &= S_{2323}^{(r)} = \frac{1}{2}. \quad (\text{B-5})
\end{aligned}$$

APPENDIX C

ORIENTATION AVERAGING

Following Jakobsen et al. (2003b), to perform orientation averaging, we assume a continuous spectrum of cavity orientations but a discrete spectrum of cavity aspect ratios or shape factors. We again divide the population of cavities into new sets of cavities, each set labeled by $j = 1, \dots, J$ and characterized by a common aspect ratio $\alpha^{(j)}$, porosity $v^{(j)}$, and orientation distribution function (ODF) $O^{(j)} \times (\Omega)$. For any (tensorial) quantity $\mathbf{A}^{(r)}$ that depends on the orientation/shape index r , we may let

$$\sum_{r=1}^N \phi^{(r)} \mathbf{A}^{(r)} \rightarrow \sum_{j=1}^J v^{(j)} \bar{\mathbf{A}}^{(j)}, \quad (\text{C-1})$$

where

$$\bar{\mathbf{A}}^{(j)} = \int d\Omega O(\Omega) \mathbf{A}(\alpha^{(j)}, \Omega). \quad (\text{C-2})$$

Here, $\bar{\mathbf{A}}^{(j)}$ represents the orientation average of $\mathbf{A}(\alpha^{(j)}, \Omega)$ and Ω symbolizes the three Euler angles that determine the orientation of the cavity relative to the crystallographic axes of the material with properties given by $\mathbf{C}^{(0)}$. For a discussion about normalization issues and correlation functions and for details about implementing the above formulas for the general case with arbitrary ODFs and the special case of transversely isotropic ODFs, see Jakobsen et al. (2003b).

REFERENCES

- Agersborg, R., M. Jakobsen, B. O. Ruud, and T. A. Johansen, 2007, The effects of pore fluid pressure on the seismic response of a fractured carbonate reservoir: *Studio Geophysica et Geodaetica*, **51**, 89–118.
- Agersborg, R., T. A. Johansen, M. Jakobsen, J. Sothcott, and A. Best, 2008, Effects of fluids and dual-pore systems on pressure-dependent velocities and attenuations in carbonates: *Geophysics*, **73**, no. 5, N35–N47.
- Auld, B. A., 1990, *Acoustic fields and waves in solids*: Krieger Publishing Company.
- Biot, M. A., 1956, Theory of propagation of elastic waves in a fluid-saturated porous solid—I: Low-frequency range: *Journal of the Acoustical Society of America*, **28**, 168–178.
- , 1962, Mechanics of deformation and acoustic propagation in porous media: *Journal of Applied Physics*, **33**, 1482–1498.
- Brown, R. J. S., and J. Korrington, 1975, On the dependence of the elastic properties of a porous rock on the compressibility of the pore fluid: *Geophysics*, **40**, 608–616.
- Carcione, J., 2007, *Wave fields in real media: Wave propagation in anisotropic, anelastic, porous and electromagnetic media*: Elsevier Science.
- Chakraborty, A., 2008, Prediction of negative dispersion by a nonlocal poroelastic theory: *Journal of the Acoustical Society of America*, **123**, 56–67.
- Chapman, M., 2003, Frequency-dependent anisotropy due to meso-scale fractures in the presence of equant porosity: *Geophysical Prospecting*, **51**, 369–379.
- Chapman, M., S. V. Zatsepin, and S. Crampin, 2002, Derivation of a microstructural poroelastic model: *Geophysical Journal International*, **151**, 427–451.
- Dvorkin, J., G. Mavko, and A. Nur, 1995, Squirt flow in fully saturated rocks: *Geophysics*, **60**, 97–107.
- Dvorkin, J., and A. Nur, 1993, Dynamic poroelasticity: A unified model with the squirt and the Biot mechanisms: *Geophysics*, **58**, 524–533.
- Eshelby, J. D., 1957, The determination of the elastic field of an ellipsoidal inclusion, and related problems: *Proceedings of the Royal Society of London*, **A241**, 376–396.
- Gassmann, F., 1951, Über die Elastizität poroser Medien: *Vierteljahrsschrift der Naturforschenden Gesellschaft in Zürich*, **96**, 1–23.
- Gueguen, Y., and V. Palciauskas, 1994, *Introduction to the physics of rocks*: Princeton University Press.
- Hudson, J. A., E. Liu, and S. Crampin, 1996, The mechanical properties of materials with interconnected cracks and pores: *Geophysical Journal International*, **124**, 105–112.
- Jakobsen, M., 2004, The interacting inclusion model of wave-induced fluid flow: *Geophysical Journal International*, **158**, 1168–1176.
- , 2007, Effective hydraulic properties of fractured reservoirs and composite porous media: *Journal of Seismic Exploration*, **16**, 199–224.
- Jakobsen, M., and J. A. Hudson, 2003, Visco-elastic waves in rock-like composites: *Studio Geophysica et Geodaetica*, **47**, 793–826.
- Jakobsen, M., J. A. Hudson, and T. A. Johansen, 2003a, *T*-matrix approach to shale acoustics: *Geophysical Journal International*, **154**, 533–558.
- Jakobsen, M., and T. A. Johansen, 2005, The effects of drained and undrained loading on visco-elastic waves in rock-like composites: *International Journal of Solids and Structures*, **42**, 1597–1611.
- Jakobsen, M., T. A. Johansen, and C. McCann, 2003b, The acoustic signature of fluid flow in complex porous media: *Journal of Applied Geophysics*, **54**, 219–246.
- Klimentos, T., and C. McCann, 1988, Why is the Biot slow compressional wave not observed in real rocks?: *Geophysics*, **53**, 1605–1609.
- Mavko, G., and D. Jizba, 1991, Estimating grain-scale fluid effects on velocity dispersion in rocks: *Geophysics*, **56**, 1940–1949.
- Mavko, G., and A. Nur, 1975, Melt squirt in the asthenosphere: *Journal of Geophysical Research*, **80**, 1444–1448.
- Mukerji, T., and G. Mavko, 1994, Pore fluid effects on seismic velocity in anisotropic rocks: *Geophysics*, **59**, 233–244.
- Mura, T., 1982, *Micromechanics of defects in solids*: Martinus Nijhoff.

- O'Connell, R. J., and B. Budiansky, 1977, Viscoelastic properties of fluid-saturated cracked solids: *Journal of Geophysical Research*, **82**, 5719–5735.
- Pointer, T., E. Liu, and J. A. Hudson, 2000, Seismic wave propagation in cracked porous media: *Geophysical Journal International*, **142**, 199–231.
- Ponte, Castañeda P., and J. R. Willis, 1995, The effect of spatial distribution on the effective behavior of composite materials and cracked media: *Journal of the Mechanics and Physics of Solids*, **43**, 1919–1951.
- Tod, S. R., 2001, The effects on seismic waves of interconnected nearly aligned cracks: *Geophysical Journal International*, **146**, 249–263.
- Tod, S. R., and E. Liu, 2002, Frequency-dependent anisotropy due to fluid flow in bed limited cracks: *Geophysical Research Letters*, **29**, 1749–1752.